A New Species of *Schizaspidia*, with Discussion of the Phylogenetic Utility of Immature Stages for Assessing Relationships Among Eucharitid Parasitoids of Ants

JOHN M. HERATY,[1,2] JASON MOTTERN,[1] and CHRISTIAN PEETERS[3]

Ann. Entomol. Soc. Am. 108(5): 865–874 (2015); DOI: 10.1093/aesa/sav062
Published online July 11, 2015

ABSTRACT Because of problems of rarity, sampling bias, and general lack of informative characters, immature stages of parasitic Hymenoptera are seldom used to resolve phylogenetic relationships. However, the ant-parasitic Eucharitidae are an exception. The adults and immature stages of *Schizaspidia diacammae* **n. sp.** (Eucharitidae: Eucharitinae: Eucharitini) are described from collections of cocooned pupae of its ant host, *Diacamma scalpratum* (Smith) (Formicidae: Ponerinae: Ponerini), in Thailand. Additional collections of planidia and pupae of *Schizaspidia nasua* (Walker) from *Odontomachus rixosus* (Smith) (Ponerini) and related Eucharitini suggest a high degree of conservatism in larval morphology across a monophyletic group of ant parasitoids that attack Ponerinae, Ectatomminae, and Myrmeciinae (PEM Clade). Pupae are especially informative, having peculiar bladder-like processes projecting from the ocelli, dorsal mesoscutellum, and laterally from the abdominal tergites. There are also a set of unusual sclerotized bars found laterally on the basal metasomal tergite. Such processes are unknown elsewhere in Hymenoptera. These same pupae offer further insights into the development of the scutellar spines. Based on a molecular analysis of relationships within the PEM Clade, we propose that scutellar spines have evolved multiple times within the group and across Eucharitidae.

KEY WORDS Hymenoptera, Chalcidoidea, Eucharitidae, Formicidae

Within Chalcidoidea, immature stages have rarely been explored for their phylogenetic utility. The lack of general information across taxa is likely the greatest impediment, with descriptive information compiled for unrelated taxa. Late-instar larvae are usually sac-like with little body ornamentation, although characters of the mandibles and head capsule can be informative for some Eurytomidae, Pteromalidae, and Torymidae (Gómez et al. 2008, 2012; Gómez and Nieves-Aldrey 2012). In contrast, the first-instar larvae and pupae can be highly ornate and have characteristics that may define major clades (Clausen 1940). Perilampidae and Eucharitidae are a demonstrably monophyletic group (Heraty et al. 2013) characterized by the sclerotized first-instar larvae (planidia), which also have characters valuable for defining relationships within the group (Clausen 1940, Heraty and Darling 1984, Darling and Roberts 1999).

All known Eucharitidae are parasitoids of the immature stages of ants. Larval stages were first described by Wheeler (1907) for *Orasema* Cameron. The late-instar larvae and pupae of Eucharitinae and Oraseminae were then described in a series of early papers summarized by Clausen (1940). The first-instar larvae are highly conservative in their morphology, but lat-instars can be strikingly ornate with numerous odd protuberances and swellings over the body. While their descriptions are sporadic, these late-instar larvae and pupae of Eucharitidae offer numerous characters useful in determining higher-level relationships. Characters of the pupal and adult stages are often correlated, especially with regard to the highly ornate posterior scutellar processes. However, we have discovered several other structures that are unique to the pupa. Derived features of the planidia, later instars, and pupae are almost invariant across higher level groups, making them very useful for assessing phylogenetic relationships (Heraty 1994, 2002).

Another oddity of Eucharitidae is the inverse evolutionary association with their ant hosts. Phylogenetic results based on molecular data suggest that the more ancestral eucharitid lineages are associated with more derived groups of ants (e.g., Formicinae and Myrmicinae), and the more derived eucharitid lineages attack the more primitive groups (e.g., Ponerinae) (Murray et al. 2013). An exemplary group is the derived eucharitid clade that attacks Ponerinae, Ectatomminae, and Myrmeciinae, termed the PEM Clade of Murray et al. (2013). Monophyly of the PEM Clade has been consistently supported in molecular analyses (Heraty et al. 2004, Murray et al. 2013), but the clade was either monophyletic or paraphyletic in analyses of adult morphological characters (Heraty 2002). The PEM Clade

[1] Department of Entomology, University of California, Riverside, CA 92521.
[2] Corresponding author, e-mail: john.heraty@ucr.edu.
[3] Institut d'Écologie et Sciences de l'Environnement, UMR CNRS 7818, Université Pierre et Marie Curie, 7 quai Saint Bernard, Paris.

can be further subdivided into three monophyletic groups that include the Chalcura and Schizaspidia Clades (Old World) and the Kapala Clade (New World; Heraty 2002, Murray et al. 2013). Several larval features offer strong support for monophyly of the PEM Clade, in accordance with Murray et al. (2013), although within the clade, they are relatively invariant. Herein we describe a new species of *Schizaspidia* attacking *Diacamma*, describe the morphology of the immature stages of two species, and discuss their relevance in justifying monophyly of PEM Clade. We also document the growth pattern of the scutellar spines in the pupa of *S. nasua*, and discuss the independent derivation of scutellar spines across Eucharitidae and within the PEM Clade using the results of a molecular analysis of relationships.

Materials and Methods

Terms for adults follow Heraty (2002) and Heraty et al. (2013). Terms for planidia follow Heraty and Darling (1984) and Heraty (2002). Species used in the descriptions and analyses were primarily identified using Hedqvist (1978) and Heraty (1998, 2002). Specimens are deposited in the Entomological Research Museum of the University of California, Riverside (UCRCENT). Photographs were taken using a Leica Imaging System with a Z16 APO A microscope and a 1.4 megapixel CCD camera (model LW1165C; Lumenera Corp., Ottawa, ON, Canada), and stacked using Zerene Stacker (version 1.04, Zerene Systems, LLC). For *Schizaspidia diacammae*, DNA was extracted from a whole pupa using the Qiagen DNeasy Blood and Tissue Kit (Qiagen, Valencia, CA) following the manufacturer's protocols, and then sequenced for 28S-D2 following the protocols outlined in Murray et al. (2013). The mature larva dissolved in the process of extraction, and the holotype female is considered the secondary voucher. The sequence was analyzed with a subset of PEM Clade taxa by Murray et al. (2013; GenBank numbers and locality information therein). The matrix consisted of 31 representatives of *Austeucharis* Bouček, *Chalcura* Kirby and *Tricoryna* Kirby (Chalcura Clade; outgroup), six *Dilocantha* Shipp (Kapala Clade), and 31 *Ancylotropus* Cameron, *Eucharissa* Westwood, *Pogonocharis* Heraty, *Saccharissa* Kirby, *Schizaspidia* Westwood, *Thoracanthoides* Girault, and an undescribed African genus near *Ancylotropus* (Schizaspidia Clade). The 28S sequences were realigned using MAFFT E-INS-i (Katoh et al. 2005) and analyzed either for 28S-D2 alone or in combination with 28S-D2-D5, COI, and COII (after Murray et al. 2013). Parsimony analyses were done using PAUP 4.0a136 (Swofford 2002), and likelihood analyses conducted using RAxML (Stamatakis et al. 2008) and MrBayes (Ronquist and Huelsenbeck 2003) through the CIPRES Portal Gateway (www.phylo.org/portal2). Results are presented for the PAUP analysis, which was based on a search of 100 random starting trees, collapse of zero-length branches, and a successive weighting analysis using the retention index scaled to 1,000, and with the resulting SAW trees reweighted to 1 and compared in length to the MP tree (cf. Heraty et al. 2004). The shape of the posterior scutellar processes (Character 50, Heraty 2002) was mapped onto the topology using Mesquite v.2.75 (Maddison and Maddison 2012).

Nomenclature. This article and the nomenclatural act it contains have been registered in ZooBank (www.zoobank.com), the official register of the International Commission on Zoological Nomenclature. The LSID (Life Science Identifier) number is: urn:lsid:zoobank.org:act:4F975359-3D02-4E83-B649-1E8122530206.

Schizaspidia diacammae n. sp.
(Figs. 1–18)

Diagnosis. Readily distinguished from species of *Pogonocharis*, *Schizaspidia*, and *Saccharissa* by the dorsoventrally flattened and laterally curved scutellar spines (Figs. 2 and 4); longitudinally carinate scutellar disc (scd); antenna 14-segmented, in females with the basal flagellomere dorsally serrate (Figs. 1, 15, and 16) or in males with the short dorsal branch (db) 1.5 times as long as basal width (fbw) of the flagellomere (Fig. 7); following flagellomeres of both sexes, except apical flagellomere pectinate, with stout, flattened branches that become longer to flagellomeres 6–7 and then shorter toward the apex (Figs. 15 and 16); face nearly smooth with weak vertical striae; fore wing with a dark medial band of infuscation that is darkest around stigmal vein (Fig. 8), and ovipositor acicular. This species would key to *Schizaspidia furcifera* Westwood in Hedqvist (1978), but as in all other *Schizaspidia*, *S. furcifera* has only 12 antennal segments, serrate flagellomeres in the female, and the scutellar spines are narrow and longitudinally carinate basally (cf. Hedqvist 1978). *Schizaspidia batuensis* Hedqvist has similar wide flattened scutellar spines, but 10 antennal flagellomeres. *Saccharissa* have 11–13 antennal segments. The excess number of flagellomeres is unusual in the tribe Eucharitini.

Female. Length 4.7–5.2 mm. Head black with dark green reflections. Mesosoma dorsally mostly greenish black except dark purple black on scutellar spines and medially on scutellar disc, lateral mesosoma, and petiole dark bluish green. Metasomal tergites dark brown with faint metallic reflections (Figs. 1 and 2). Antennal scape white, pedicel pale brown, flagellum brown. Mandibles and labrum pale brown (Fig. 6). Coxae brown to black, remaining leg segments white, with apex of terminal tarsomere brown. Wings mostly hyaline, fore wing with broad infuscate cloud extending from marginal vein across wing disc, darkest around stigmal vein (Fig. 8). Fore wing venation dark brown beyond submarginal vein, which is lighter in color. Hind wing venation brown but lighter basally and distally.

Head 1.38–1.42 times as broad as high (Fig. 5). Upper frons mostly smooth but with weak vertical striae and laterally directed appressed setae; lower face smooth and shining with sparse appressed setae; supraclypeal area smooth and bare; clypeus smooth with few scattered seta dorsally and a medial patch of erect setae just above clypeal margin and on the anteclypeus;

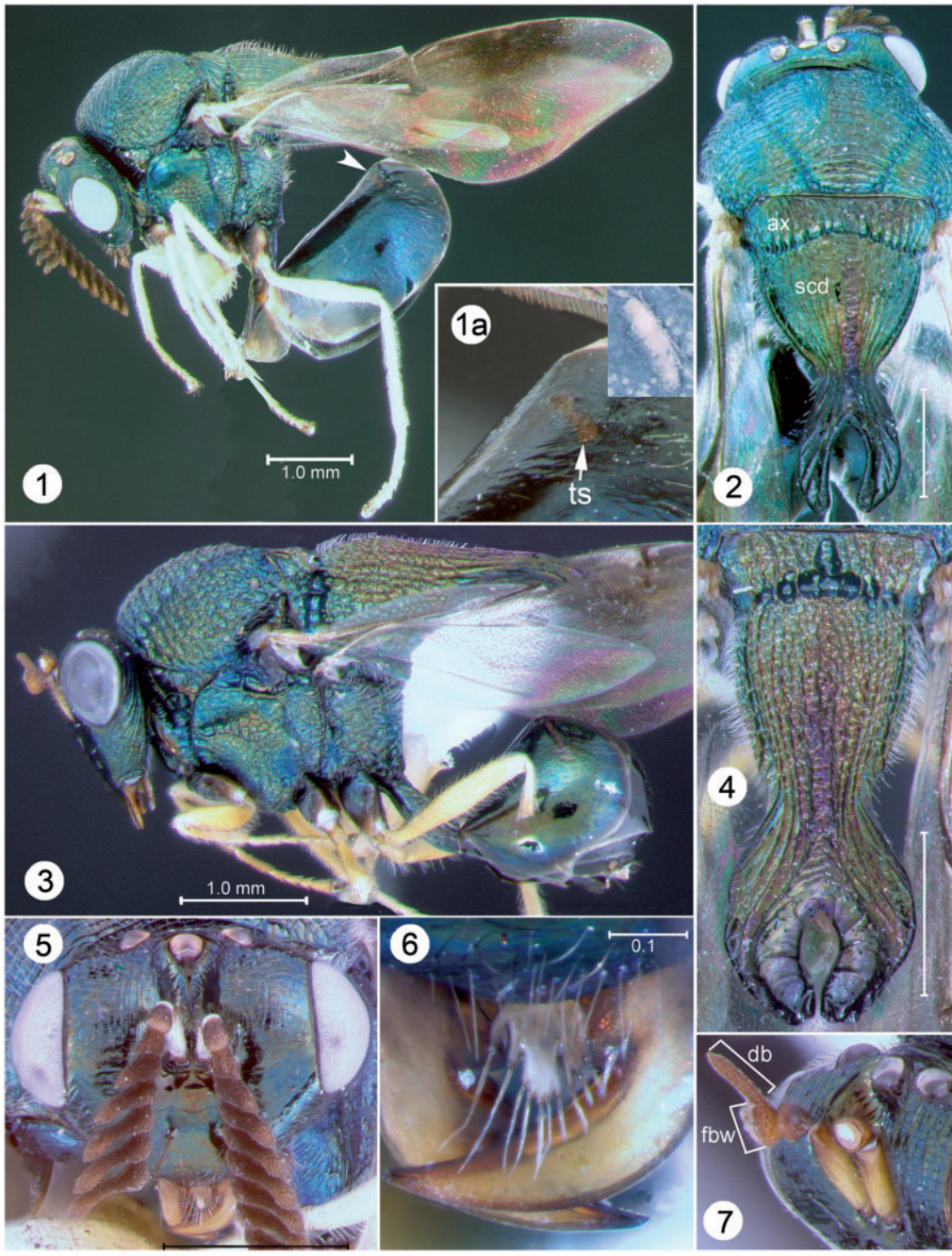

Figs. 1–7. *S. diacammae*. (1) Female, habitus, arrow pointing to area of inset enlargement, 1a, tergal scar (ts). (2) Female, head and mesosoma, dorsal view, axilla (ax), scutellar disc (scd). (3) Male, lateral habitus. (4) Male, mesoscutellum, dorsal view. (5) Female head in frontal view. (6) Female labrum and mandibles. (7) Male head in anterolateral view, dorsal branch (db), flagellomere basal width (fbw).

anteclypeus distinct with a broadly rounded ventral margin. Gena obliquely striate, with striae continuous across occiput just posterior to lateral ocelli. Eyes separated by 1.38–1.4 times their height. Malar space 1.07–1.25 times the height of the eye, malar depression or sulcus absent. Mandibles robust and 3/2 dentate, apical tooth reaching opposing genal area. Labrum flattened and apically incised into irregular lobes, with 10 digits, digits short but distinct laterally and indistinct medially, labral setae long and hair-like (Fig. 6). Palpomeres absent; galea long and acute, reaching as far as labral apex. Antenna 14-segmented; flagellum 12-segmented

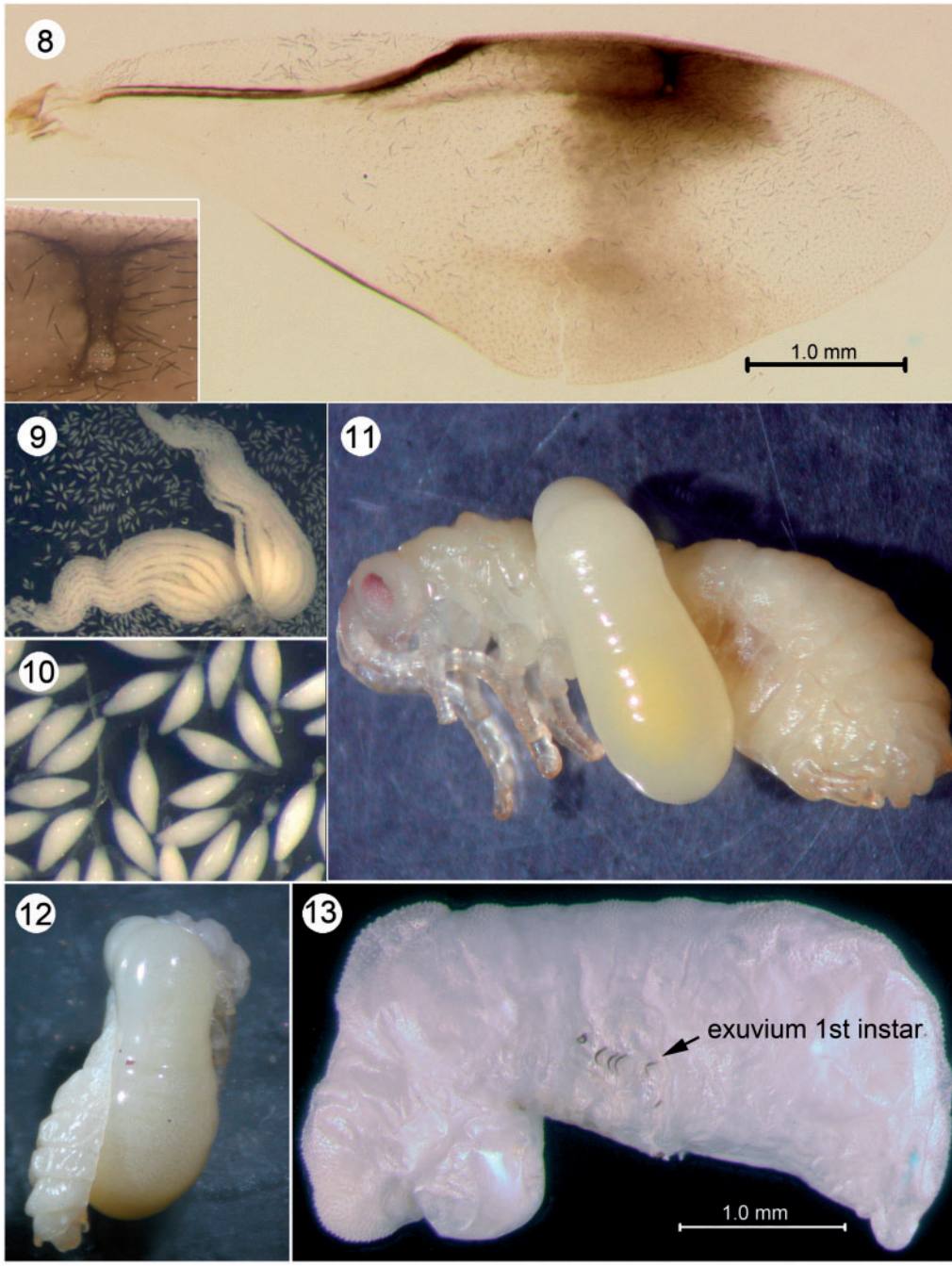

Figs. 8–13. *S. diacammae*. (8) Female fore wing, inset is magnification of stigmal vein. (9) Dissected ovaries. (10) Ovarian eggs. (11) Second-instar feeding on host. (12) Third-instar feeding on host. (13) Second instar with attached exuvium of first instar.

(from mature pupa, tips broken in adult holotype; Fig. 5); scape cylindrical with a short apico-medial carina, scape not reaching median ocellus; flagellum 1.1 times head height (from pupa; Fig. 16); basal flagellomere serrate with an acute tip dorsally, 1.0 times as long as broad, following flagellomeres approximately same length, each with a progressively longer then shorter basally flattened dorsal branch, branches arranged linearly; surface sculpture of flagellomeres finely rugulose-reticulate; apical flagellomere spherical; multiporous plate sensilla potentially absent (not visible using stereoscope).

Mesosoma dorsally costate with scattered fine setae; mid- and lateral lobes of mesoscutum transversely

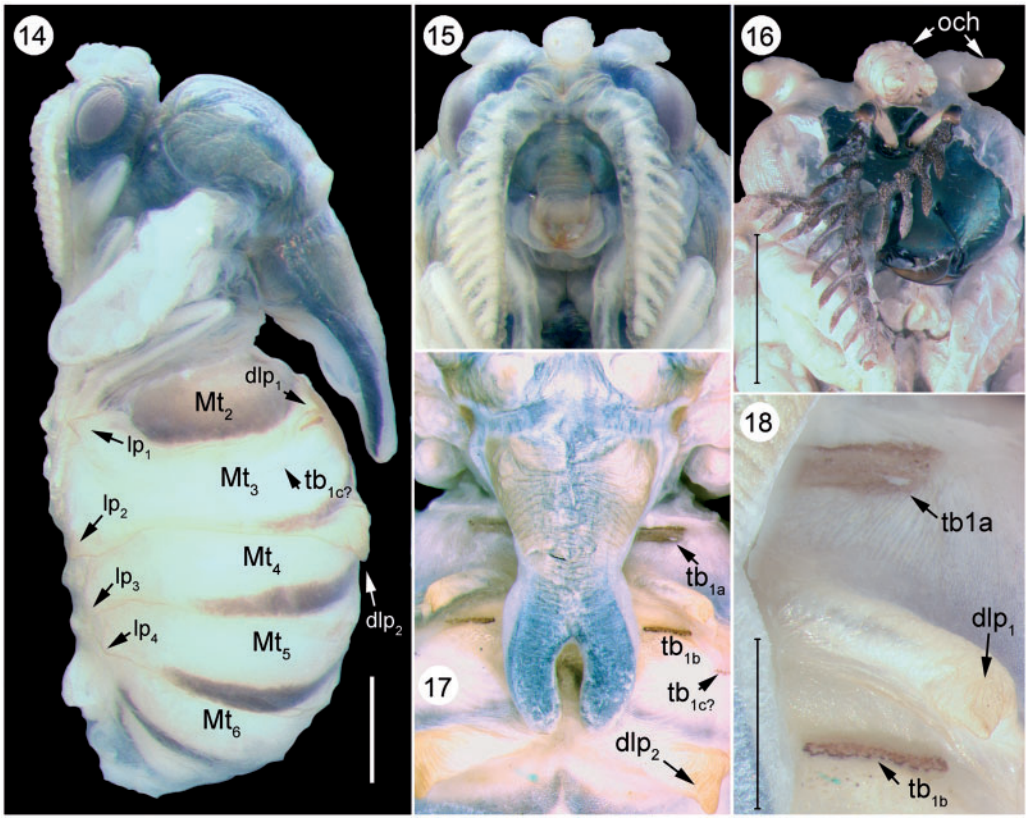

Figs. 14–18. *S. diacammae*, female pupa. (14) lateral. (15–16) head in ventral view (och = ocellar horns). (17) scutellum and basal tergites in dorsal view. (18) Magnification of metatosomal tergal bars just right of scutellar processes. Abbreviations: lp, lateral process; dlp, dorsolateral process; Mt, metasomal tergite; tb, terga bar.

costate, subcircular in dorsal view, axilla and scutellar disc longitudinally costate (Fig. 2). Scutellum 2.3–2.5 times dorsal length of mesoscutum; axillae (ax) transverse and broadly impressed medially, scutoscutellar sulcus transverse and deeply foveate (Fig. 2); scutellar disc (scd) with rugulose median channel and scd bordered laterally by sharp carinae and crenulate sulcus; scutellar spines narrower than scutellar disc, dorsoventrally flattened, obliquely costate, and with a sharp carinate lateral margin. Propodeal disc flat with fine rugulose sculpture medially and dense long setae laterally; propodeal spiracle circular with raised margin; callus and metapleuron rugose; metapleural sulcus present, extending from dorsal metacoxal articulation and joining mesepimeron at half dorsal height. Femoral groove narrowly impressed and foveate; upper mesepimeron rugulose; lower mesepimeron rugulose, but smooth posteroventrally and anterodorsally, strongly alveolate below fore wing articulation. Prepectus triangular dorsally, reaching slightly less than half distance between spiracle and tegula; upper triangle broadly impressed medially with a carinate margin, not interlocking with mesepimeron (Fig. 1). Coxae smooth, bare, and semiglobose; femora smooth and pilose; metafemur slender, 6.4 times longer than broad; calcar straight and acuminate; one metatibial spur. *Fore wing* 2.6–2.7 times as long as broad (Fig. 8); costal cell and wing disc densely setose but with basal area bare; posterior margin of wing disc with minute marginal fringe (Fig. 8), absent along anterior margin; costal cell 0.4 times as long as wing; wing veins evenly sclerotized; stigmal vein four times as long as broad and perpendicular to fore wing margin, slightly enlarged apically with anteroventral projection, with a cluster of several campaniform sensillae on the stigma (Fig. 8 inset). *Hind wing* broad and apically narrowed, hamuli composed of two straight basal spines and seven following hooked spines; disc pilose, lacking posterior fringe.

Petiole 1.1 times as long as broad in lateral view, 1.0 times as long as metacoxa, dorsally weakly rugose, with appressed setae apically. Gaster globose, first tergite (Gt_1) smooth with few short setae dorsally, tergal scar prominent and oblique (Fig. 1a). Gastral sternites smooth; hypopygium with cluster of dense hairs apically (from pupa). Ovipositor acicular.

Male. Length 4.7 mm. Coloration as in female, but scape and legs mostly pale brown, apex of femora and base of tibia more lightly colored.

Head 1.4 times as broad as high. Frons with distinct vertical striae (Fig. 7), lower face smooth. Eyes separated by 1.9 times their height. Malar space 1.2 times height of eye. Labrum with 14 marginal setae arranged on three flattened lobes (4-6-4 marginal setae), with only short labral digits on left lobe and hairs sessile on

other lobes. Antenna lost beyond basal flagellomere, which is transverse and 1.7 times as broad as long with a dorsal branch about three times as long as broad (Figs. 3 and 7).

Mesosoma as in female but with more pronounced dorsal sculpture (Fig. 4). Scutellum 2.5 times as long as midlobe of mesoscutum; scutoscutellar sulcus deeply foveate medially, posteror spines broader than scutellar disc. Coxae dark brown with dark green reflections. *Fore wing* 2.3 times as long as broad.

Petiole 2.0 times as long as broad, 1.4 times as long as metacoxa; ventral margin of petiole slightly curved in profile (Fig. 3). Gaster globose.

Etymology. Named for the ant host.

Ovarian egg (Figs. 9 and 10). Dissected ovaries revealed a large number of fully developed oocytes, suggesting that adults are proovigenic. The morphology of the ovipositor (acicular) suggests that eggs are deposited similar to *Schizaspidia convergens* (Walker), which deposit clusters of a few hundred eggs into leaf or flower buds (Clausen 1940). The ovarian eggs are similar in structure to other Eucharitidae: smooth, egg body slightly arcuate, and egg stalk present but less than half length of egg body.

First-instar (from exuvium without head capsule, Fig. 13). Tergites TI and TII fused dorsally, with four pairs of setae, ventrolateral pair as stout spines; tergopleural line (tpl) present on TII to TVIII; relative to tpl, TIII with one ventral and one dorsal pair of seta and ventral margin with one short and one long narrow spine-like extension; TIV with one dorsal pair of setae, one long ventral posteriorly directed extension and crenulate margin ventral to tpl; TV similar but the one dorsal pair of setae and one stout ventral pair; TVI as in TIV, but spine more robust; TVII with crenulate margin posterolaterally and with one long robust socketed spine on posteroventral margin; TVIII without setae but with crenulate ventral margin and long posterior extension of posterior ventral margin; TIX with pair of long bifurcating spine-like extensions from posterior ventral margin reaching to apex of TXI; TX and TXI tubular; TXII elongate with acute emarginate apex; cerci short and reaching as far as TXII apex. The elongate bifurcating extensions of TIX and short cerci are characteristic of other described *Schizaspidia* (Clausen 1940, Ishii 1932). The planidium of *Kapala* is almost identical but with the cerci as long as TXI and XII (Pérez-Lachaud et al. 2006, Fig. 13).

Second-instar *(Figs. 11 and 13).* Length 3.3–3.8 mm. Body segments excluding head with dorsal patches of minute papillae; thorax angulate in profile, swollen anteriorly above head capsule and posteriorly at angle of thorax and abdomen; one enlarged circular prothoracic spiracle opening apparent laterally just posterior to anterodorsal protuberance, remaining spiracles not apparent; exuvium of first-instar remaining attached to venter of abdomen. Observed feeding on junction of thorax and abdomen of ant host. Ant host pupa (Fig. 11) deformed, as originally described by Wheeler (1907).

Third-instar (Fig. 12). Length 5.2–6.4 mm. Similar in shape and dorsal papillate sculpture to second instar, but with dorsal anterior thoracic region more strongly protruding, as described for *S. convergens* (Clausen 1940, cf. Fig. 8), also with only prothoracic spiracle apparent; exuvium of first-instar remaining attached to venter of abdomen. *Kapala* has a similar third-instar, but the prothoracic region does not project over the head (Pérez-Lachaud et al. 2006, fig. 18). A single larva consumes virtually all of the ant host (Fig. 12).

Pupa (Figs. 14–18). Length 7.8–8.1 mm, measured from vesicular processes of head to apex of abdomen. Pupa generally conforming to shape of adult wasp. Several peculiar features of this pupa are shared with the pupa of *Austeucharis myrmiceae* (Cameron) (Brues 1919) and *Kapala izapa* Carmichael (Pérez-Lachaud et al. 2006). Head with three dorsal vesicular processes (ocellar horns) associated with each of the ocelli (Figs. 15 and 16, och), horns slightly angled ventrally, medial horn bifurcating apically into two annulated processes (Fig. 16). Metasomal terga 2–5 each have an expanded process along the ventrolateral margin (Fig. 14, $lp_{1\text{-}4}$), with similar bladder-like processes dorsolaterally on the first two metasomal terga (Figs. 14, 17, and 18, $dlp_{1\text{-}2}$). The first two metasomal terga also bear three dorsolateral transverse sclerotized bars ($tb_{1a\text{–}c?}$) that decrease in width from anterior to posterior. By comparison to the underlying terga in the one fully developed pupa, the anterior bar (tb_{1a}) is directly associated with the tergal scar (Fig. 1, ts), the median bar (tb_{1b}) associates with a sclerotized bar on the intersegmental membrane of the adult between Mt_1 and Mt_2, and the very narrow posterior bar (Figs. 14, 17, $tb_{1c?}$) had no visible association with the adult terga. *Austeucharis* has identical ocellar horns, and similar dorsolateral and ventrolateral vesicular abdominal processes, but with both processes on each of metasomal tergites 2–5 (Brues 1919). *Dicoelothorax platycerus* (Ashmead) (Torréns 2013, Fig. 2d), *K. izapa* (Pérez-Lachaud et al. 2006) and *Kapala* sp. (unpublished) also have ocellar horns and dorsolateral tubercles on $Mt_{3\text{–}4}$ and ventrolateral tubercles on $Mt_{2\text{-}5}$ (fewer in *K. izapa*). All of the genera with ocellar horns and abdominal tubercles belong to the PEM Clade of Eucharitidae (Murray et al. 2013). These structures are unknown elsewhere in Eucharitidae or Chalcidoidea.

Ant host: *Diacamma scalpratum* (Smith) (Ponerinae: Ponerini).

Holotype: Thailand: Phitsanulok Province: Thung Salaeng Luang NP, 16° 34′32″ N, 100° 53′01″ E, September 2006, C. Peeters, pine forest, ex *Diacamma scalpratum*, TH-4 (1♀, UCRCENT00412513). Dissected ovaries and host cocoon stored separately in ethanol (UCRCENT00435887). Deposited in UCRC. **Paratypes:** same data UCRCENT00412514 1♂ TH-5; UCRCENT00412515 sex unknown TH-5, body fragmented; UCRCENT00412519 1♀ pupa TH-5. **Additional material examined (immatures):** same data: UCRCENT00435895-6 first-instar exuvium; UCRCENT00412518 third-instar TH-5; UCRENT00435888 third-instar TH-5 (etoh); UCRCENT00412520 second-instar TH-3; UCRCENT00412521 second-instar TH-3; UCRCENT00412523 pupa TH-2; UCRCENT00412517 host remains extracted from cocoons TH-5. **Associated ant host remains:** same data but for *Diacamma*

scalpratum: UCRCENT00412516 deformed pupa TH-5; UCRCENT00412522 deformed pupa TH-3; UCRCENT00435889 TH-5, 2 deformed pupae with cocoons (etoh); UCRCENT00412524–25 cocoons, TH-3, TH-4. **TH-2–5** refers to different colony excavations.

GenBank Sequence: KP271499. Mature larva destroyed during extraction. Specimen record UCRCENT00412513 TH-4.

Schizaspidia nasua (Walker)
(Figs. 19–23)

First-instar (Figs. 19, 24, and 25). Four mature larvae of *Odontomachus rixosus* (Smith) had multiple planidia attached to the thoracic region of the host (Fig. 19). Planidia were either slightly burrowed into the host or attached superficially (Fig. 19 inset). Planidium (Figs. 24 and 25) as in *S. diacammae*, but with cerci as long as TXI–XII.

Pupa (Figs. 20–23). Length ♀ 3.71–5.76 mm (4.62 ± 0.66), ♂ 2.90–6.05 (4.39 ± 0.91). Pupa as described for *S. diacammae*, but with additional pair of vesicular processes on dorsum of mesoscutellum over axillula (as in *D. platycerus*, Torréns 2013), and abdomen dorsally with only one pair of posterior bladders, and ventrolateral tubercles on $Mt_{2\text{-}5}$, with the last process only weakly developed; cuticular bars (tb_{1a} and tb_{1b}) present but weakly sclerotized (Fig. 23); $tb_{1c?}$ not apparent. One pupa found in an early stage of development had the body mostly formed, with the protuberances (och and msp) developed but not erect, and the scutellar spines had not begun to develop (Fig. 20). The scutellar processes appear to be the last structure to develop on the maturing pupae (Fig. 21), with the spines fully developed when the pupa was fully sclerotized (Figs. 22 and 23).

Ant Host: *Odontomachus rixosus* Smith (Ponerinae: Ponerini).

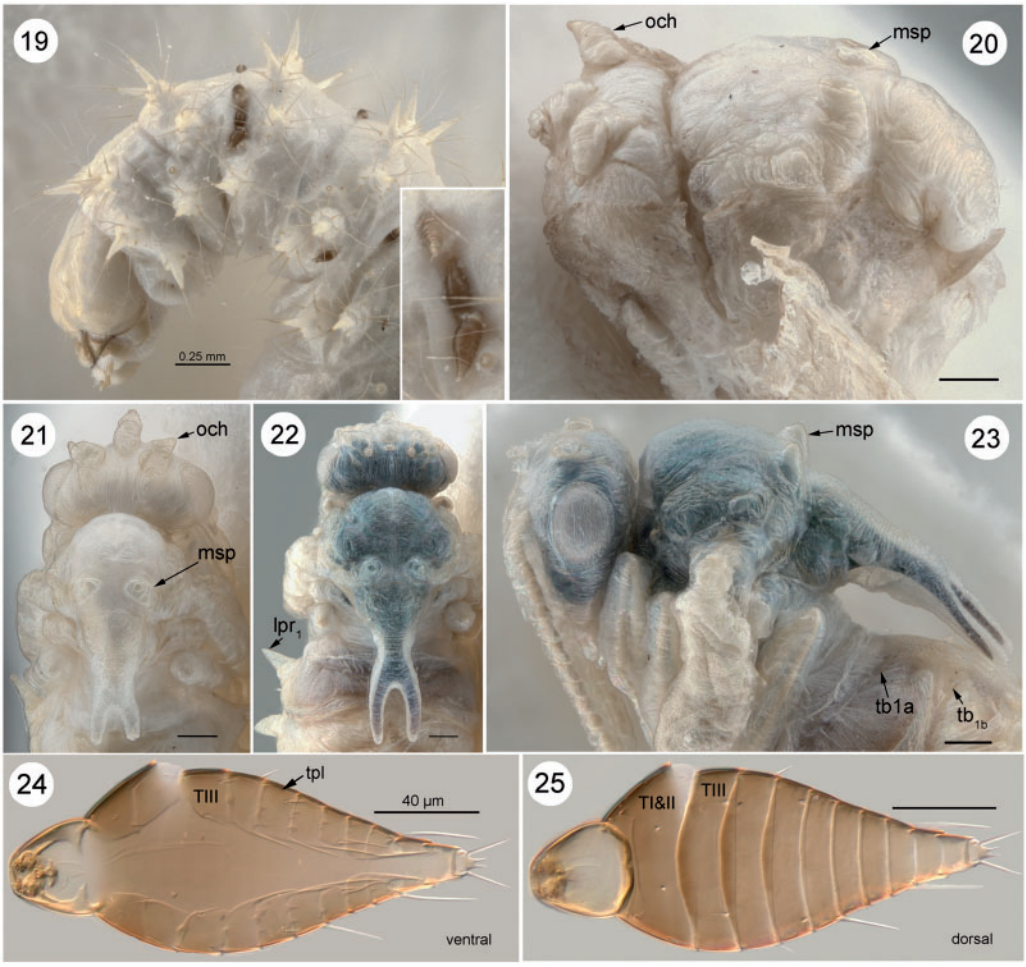

Figs. 19–25. *Schizaspidia nasua*. (19) *Odontomachus* larva with multiple plandia, inset is enlargement of planidia. (20) Undeveloped pupa partially encased by host remains, spines not yet developed. (21) Male pupa, dorsal view, partially developed with spines elongating. (22–23) Female pupa, dorsal view, adult fully developed: 22, dorsal view; 23 lateral view. (24–25) First instar: 24, ventral view; 25, dorsal view. Abbreviations: lp, lateral process; msp, mesoscutellar process; och, ocellar horn; T, tergite; tb, terga bar, tpl, tergopleural line.

Material Examined: **West Malaysia: Negri Sembilan:** Pasoh Forest Reserve, 2° 58′56″ N, 102° 18′20″ E, 24–I–1991, Roscizewski, rotten wood, ex: *Odontomachus rixosus* (3♂ adults, 1? adult [broken], 29♂ pupae, 23♀ pupae, 4 ant larvae with planidia; UCRC: UCRCENT00435815–74, 2 planidia UCRCENT00435886, 890). Ant hosts: (7♀, 1 pupa [psithergate], 1 larva, UCRC: UCRCENT00435875–83).

Results and Discussion

Parsimony analysis of the PEM Clade using the four gene data set recovered 285 trees (1,513 steps, RI 74), with successive weighting reducing this set to seven trees of the same unweighted length (Fig. 26), thus the results were stable to successive approximations (Carpenter 1988, Heraty et al. 2004). In both parsimony and likelihood results, *S. diacammae* grouped with *Pogonocharis* and *Schizaspidia* (BS: 87% parsimony, 97% likelihood), with *Saccharissa* consistently monophyletic and separated from this clade by *Thoracanthoides*. In parsimony and Bayesian results, the relationships of *Pogonocharis*, *Schizaspidia* and *S. diacammae* were unresolved (Fig. 26). In the likelihood (RAxML) results, *S. diacammae* was grouped with *Pogonocharis* with strong support (84% BS) and sister to *Schizaspidia* (74% BS). Given the limited taxon sampling within each of these taxa, we regard the unresolved parsimony hypothesis as best representing the current results. Based on these results and the morphological discussion above, we allocate *S. diacammae* to *Schizaspidia*.

Based on the 14-segmented antennae and a long, straight stigmal vein perpendicular to the fore wing margin (Fig. 8 inset), we initially placed *S. diacammae* in *Saccharissa*. However, the flattened, laterally carinate scutellar processes (Figs. 2 and 4) are more similar to those of *Pogonocharis* and *Schizaspidia*. In addition, *S. diacammae* lacks the prominent lateral projections of the mesoscutum over the tegula and prominent swelling of the femora that are characteristic of *Saccharissa* (Heraty 2002). No other *Schizaspidia* are known to have more than 12 antennal segments, and the female antennal flagellum is at most strongly serrate and never pectinate (Hedqvist 1978, Heraty 2002). *Pogonocharis* are distinguished by the lack of antennal branches and several other attributes (Heraty 2002). Within the *Schizaspidia* Clade, these three genera (*Pogonocharis*, *Saccharissa*, and *Schizaspidia*) were proposed to be monophyletic based on sharing basally joined and apically forked scutellar spines, three-segmented palpi, and lack of an intertorular ridge (Heraty 2002). *Schizaspidia* and *Saccharissa* were proposed as sister groups based on the pectinate male antennae with a differentiated basal flagellomere (cylindrical to short branched) and a prominent axillular groove bordering the scutellar disc. Heraty (2002) suggested that the monophyly of *Saccharissa* was problematic, and potentially this rendered *Schizaspidia* paraphyletic. In the molecular analyses of Murray et al. (2013), *Pogonocharis* and *Schizaspidia* were sister groups, and *Saccharissa* was sister to *Ancylotropus carniscutis* Cameron. Our results are similar in that *Pogonocharis* and *Schizaspidia* are sister groups (Fig. 26). *Saccharissa* are not sister group to *Ancylotropus*, but they are separated from *Schizaspidia* by *Thoracanthoides*.

Within Eucharitini, the basal flagellomere (anellus in other Eucharitidae) is absent (Heraty 2002), and most included taxa have ≤10 flagellomeres. More than 10 flagellomeres are known to occur in some species of *Eucharis* (Eucharis Clade), *Eucharissa*, *Saccharissa*, *S. diacammae* (Chalcura Clade), and *Carletonia* (sister to Kapala Clade; Heraty 2002). Our results, and those of Murray et al. (2013), would suggest that additional segments beyond 10 are derived at least four times in Eucharitinae. Among the PEM Clade taxa (cf. Fig. 26), dorsal branches on the male antennal flagellum are variably present in both the Chalcura and Schizaspidia Clades, but are found in all members of the New World *Carletonia* and the Kapala Clade. Within the Schizaspidia Clade, dorsal branches are absent only in *Ancylotropus*, the New Genus (Ethiopian) that is close to *Ancylotropus* and *Pogonocharis*. Within the Schizaspidia Clade, our results support the single evolution of ramose male antennae within the Saccharissa-Schizaspidia Clade, with subsequent loss in *Pogonocharis*.

Within Eucharitidae, extended posterior mesoscutellar processes (spines) are known only in Akapalinae and Eucharitini. The shape of these processes was partitioned by Heraty (2002) into nine different states, with a focus on their scutellar origin, degree of separation basally, and apical development. Posterior spines are independently developed to some degree in each of the major groups of Eucharitini (Heraty 2002, Murray et al. 2013), with some of the most extreme forms occurring in the PEM Clade (Fig. 26). Spines are absent in the Chalcura Clade. Among the New World PEM genera, *Carletonia* has an extended scutellar apex (character 50: state 1 in Heraty 2002), *Colocharis* has short bifurcating spines, and the remaining members of the Kapala Clade have long basally bifurcating processes/spines (state 5; Fig. 26-2265). Within the Schizaspidia Clade, there is a more diverse pattern of spine development. Complete absence (state 0) of any posterior process occurs in both *Eucharissa* and *Ancylotropus montanus*. Species of the new genus from Africa (similar to *Ancylotropus*) have a process that varies from a short flattened extension (Fig. 26-0157) to a broad bifurcating spine similar to *S. diacammae* (none included in analysis). One of the most common Asian species, *A. carniscutis*, has a single elongate spine with a truncate or emarginate apex (state 3; Fig. 26-2836a) that is similar to the extreme form of *Saccharissa alcocki* (Fig. 26-2032). *Ancylotropus ivondroi* (Risbec) (Fig. 26-0627) has a short bifurcating spine that might be considered close to that of *Schizaspidia* (state 3), but also is similar to unrelated genera within the Stilbula Clade. *Saccharissa vicina* (Masi) (state 3) has a weakly bifurcating process (Fig. 26-1592) that is similar to both *S. alcocki* and other state 3 genera (*Pogonocharis* and *Schizaspidia*), but always lacking a pronounced bifurcating apex. *Thoracanthoides* (Australia) has an acicular scutellar processes (state 8) that is more similar to unrelated members of the Eucharis Clade. The posterior process of *Schizaspidia* and *Pogonocharis*

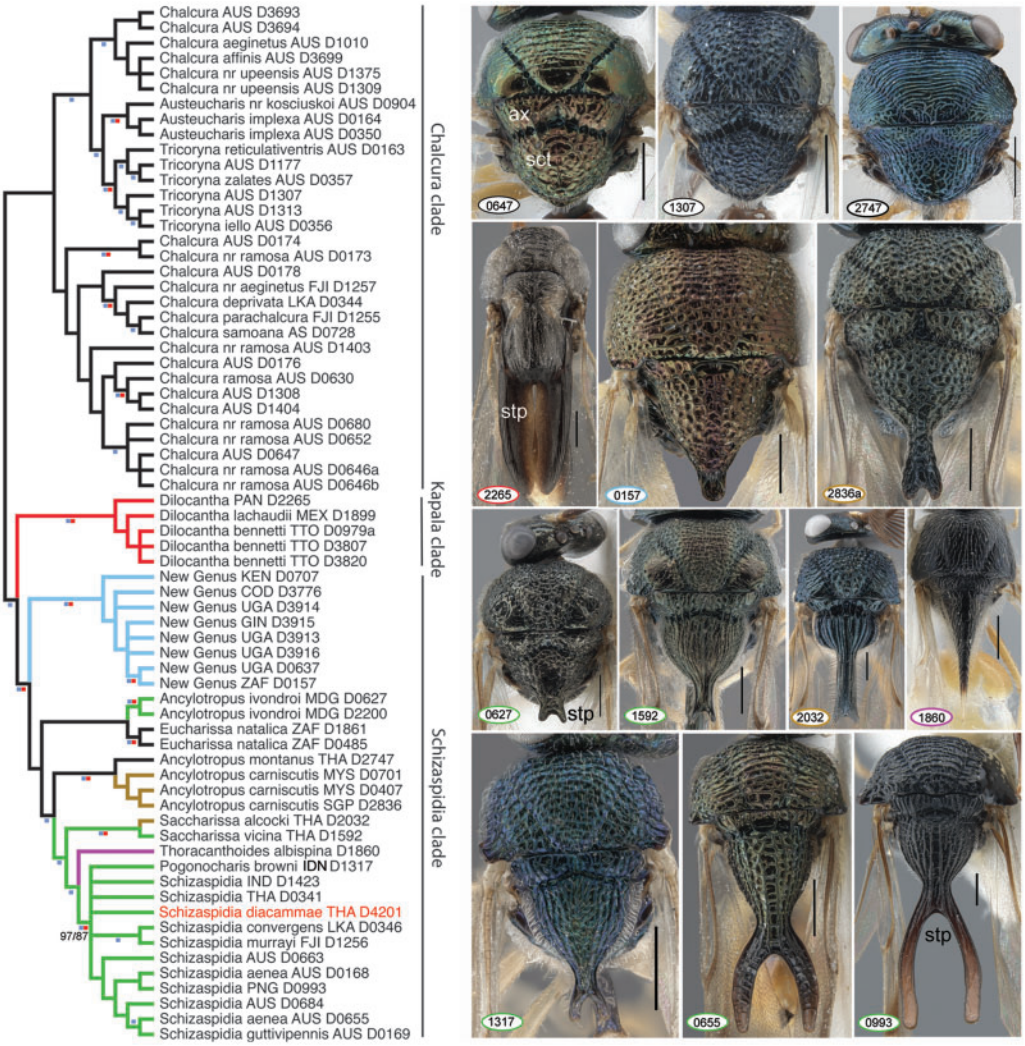

Fig. 26. Strict consensus parsimony tree (1,513 steps, RI 0.74, 150 trees) for 18S, 28S D2-D5, COI and COII. Colored branches based on state changes for character 50 in Heraty (2002): black = no scutellar projection (state 0); blue = apical margin slightly produced (state 1); brown = cylindrical process with truncate apex (state 3); green = projection forked and flattened with lateral carina (state 4); purple = single long apical process (state 8). Blue (likelihood) and red (unweighted parsimony) boxes associated with branches indicate bootstrap support greater than 80%. Images of the mesosoma (dorsal) to right correspond to DNA vouchers on cladogram (2836 replaced by image of secondary voucher). Abbreviations: ax, axilla; sct, mesoscutellar disc; stp, scutellar process. Scale bars are 0.5 mm. Country abbreviations: AS, American Samoa; AUS, Australia; COD, Republic of Congo; FJI, Fiji; GIN, Guinea; IDN, Indonesia; IND, India; KEN, Kenya; LKA, Sri Lanka; MDG, Madagascar; MYS, Malaysia; PAN, Panama; PNG, Papua New Guinea; SGP, Singapore; THA, Thailand; TTO, Trinidad; UGA, Uganda; ZAF, South Africa. Countries followed by UCR DNA voucher codes.

(state 3) are similar, with a common scutellar base and a flattened, bifurcating and laterally carinate apex (Fig. 26-1317, 0655, 0993). An even greater range of scutellar-process morphology for *Schizaspidia* is diagrammed in Hedqvist (1978). The lack of any spine in *Eucharissa*, *A. montanus* and the outgroup (Chalcura Clade and *Carletonia*) suggests that lack of spines is plesiomorphic within the clade. Within the Schizaspidia Clade, extreme scutellar processes have developed at least five times (Fig. 26). Across the PEM Clade, the posterior processes appear to have developed only one other time all species of the Kapala Clade.

There is no verified function for the posterior scutellar processes. These occur across the tribe Eucharitini. While they are unknown in the more basal Eucharitidae (Gollumiellinae, Oraseminae, and Psilocharitini), they are present and well developed in Akapalinae, which is the proposed sister group to the remaining Eucharitidae (Heraty et al. 2013). Within Eucharitini, the behavior of ants physically removing eucharitids from the ant nest upon emergence has been observed several times (Ayre 1962, Howard et al. 2001, Buys et al. 2010, Lachaud and Pérez-Lachaud 2012, Pérez-Lachaud et al. 2015). Both Lachaud and Pérez-Lachaud (2012, c.f. Fig 2g)

and Pérez-Lachaud et al. (2015, c.f. Supplementary Video 3) document how *Ectatomma* can pick up and transport adults of *Kapala* (related members within Eucharitini) by their scutellar spines. Given the aggressive behavior of these ants, the spines may protect the wings during specimen transport out of the nest, and might account for their independent development in different Euchairitini, but this has never been studied. Based on our limited observations of *S. nasua*, the extension and development of these posterior processes are one of the last stages in development of the host pupa. Additional structures such as the ocellar horns (Figs. 14–16), transverse bars in the pupa (Figs. 14, 16, and 17) and their associated external representation of tergal scars in the adult (Fig. 1, 1a), and bladder-like processes on the mesoscutum and the lateral tergites occur only in the eucharitid clade attacking Ponerinae, Ectatomminae, and Myrmeciinae. These derived features offer very strong support for the monophyly of the PEM Clade. Future studies of the behavioral interactions of these eucharitids with their ant hosts may help to resolve the function of these bizarre structures.

Acknowledgments

Many thanks to Krzysztof Roscizewski for the collection of *Schizaspidia nasua* brood. Austin Baker, Krissalyn Dominguez, John Hash, Judith Herreid, and Scott Heacox offered constructive comments on the manuscript. This research was supported in part by National Science Foundation grant DEB 1257733 to J.M.H.

References Cited

Ayre, G. L. 1962. *Pseudometagea schwarzii* (Ashm.) (Eucharitidae: Hymenoptera), a parasite of *Lasius niger* Emery (Formicidae: Hymenoptera). Can. J. Zool. 40: 157–164.

Buys, S. C., R. Cassaro, and D. Salomon. 2010. Biological observations on *Kapala* Cameron 1884 (Hymenoptera Eucharitidae) in parasitic association with *Dinoponera lucida* Emery 1901 (Hymenoptera Formicidae) in Brazil. R Trop. Zool. 23: 29–34.

Carpenter, J. C. 1988. Choosing among multiple equally parsimonious cladograms. Cladistics 4: 291–296.

Clausen, C. P. 1940. The immature stages of Eucharidae (Hymenoptera). J. Wash. Acad. Sci. 30: 504–516.

Darling, D. C., and H. Roberts. 1999. Life history and larval morphology of *Monacon* (Hymenoptera: Perilampidae), parasitoids of ambrosia beetles (Coleoptera: Platypodidae). Can. J. Zool. 77: 1768–1782.

Gómez, J. F., and J. L. Nieves-Aldrey. 2012. Notes on the larval morphology of Pteromalidae (Hymenoptera: Chalcidoidea) species parasitoids of gall wasps (Hymenoptera: Cynipidae) in Europe. Zootaxa 3189: 39–55.

Gómez, J. F., J. L. Nieves-Aldrey, and M. Hernándes-Nieves. 2008. Comparative morphology, biology and phylogeny of terminal-instar larvae of the European species of Toryminae (Hym., Chalcidoidea, Torymidae) parasitoids of gall wasps (Hym. Cynipidae). Zool. J. Linn. Soc. 154: 676–721.

Gómez, J. F., J. L. Nieves-Aldrey, M. Hernándes-Nieves, and G. N. Stone. 2012. Comparative morphology and biology of terminal instar larvae of some *Eurytoma* (Hymenoptera, Eurytomidae) species parasitoids of gall wasps (Hymenoptera, Cynipidae) in western Europe. Zoosytema 33: 287–323.

Hedqvist, K. J. 1978. Some Chalcidoidea collected in the Philippine, Bismarck and Solomon Islands. 2. Eucharitidae, with keys and check-lists to Indo-Australian genera (Insecta, Hymenoptera). Steenstrupia 4: 227–248.

Heraty, J. M. 1994. Classification and evolution of the Oraseminae in the old world, with revisions of two closely related genera of Eucharitinae (Hymenoptera: Eucharitidae). Life Sci. Contr. R. Ontario Mus. 157: 1–174.

Heraty, J. M. 1998. The genus *Dilocantha* (Hymenoptera: Eucharitidae). Proc. Entomol. Soc. Wash. 100: 72–87.

Heraty, J. M. 2002. A revision of the genera of Eucharitidae (Hymenoptera: Chalcidoidea) of the World. Mem. Am. Entomol. Inst. 68: 1–359.

Heraty, J. M., and D. C. Darling. 1984. Comparative morphology of the planidial larvae of Eucharitidae and Perilampidae (Hymenoptera: Chalcidoidea). Syst. Entomol. 9: 309–328.

Heraty, J. M., D. Hawks, J. S. Kostecki, and A. E. Carmichael. 2004. Phylogeny and behaviour of the Gollumiellinae, a new subfamily of the ant-parasitic Eucharitidae (Hymenoptera: Chalcidoidea). Syst. Entomol. 29: 544–559.

Heraty, J. M., B. D. Burks, A. Cruaud, G. Gibson, J. Liljeblad, J. Munro, J.-Y. Rasplus, G. Delvare, P. Janšta, A. V. Gumovsky, et al. 2013. A phylogenetic analysis of the megadiverse Chalcidoidea (Hymenoptera). Cladistics 29: 466–542.

Howard, R. W., G. Pérez-Lachaud, and J. P. Lachaud. 2001. Cuticular hydrocarbons of *Kapala sulcifacies* (Hymenoptera: Eucharitidae) and its host, the ponerine ant *Ectatomma ruidum* (Hymenoptera: Formicidae). Ann. Entomol. Soc. Am. 94: 707–716.

Katoh, M. Y., K. Kuma, H. Toh, and T. Miyata. 2005. MAFFT version 5: Improvement in accuracy of multiple sequence alignment. Nucleic Acids Res. 33: 511–518.

Lachaud, J. P., and G. Pérez-Lachaud. 2012. Diversity of species and behavior of hymenopteran parasitoids of ants: A review. Psyche 2012: 1–24.

Maddison, W. P., and D. R. Maddison. 2012. Mesquite Version 2.75.

Murray, E., A. E. Carmichael, and J. M. Heraty. 2013. Ancient host shifts followed by host conservatism in a group of ant parasitoids. Proc. R. Soc. 280: 20130495.

Pérez-Lachaud, G., J. M. Heraty, A. Carmichael, and J. P. Lachaud. 2006. Biology and behavior of *Kapala* (Hymenoptera: Eucharitidae) attacking *Ectatomma*, *Gnamptogenys*, and *Pachycondyla (Formicidae: Ectatomminae and Ponerinae) in Chiapas, Mexico*. Ann. Entomol. Soc. Am. 99: 567–576.

Pérez-Lachaud, G., J. C. Bartolo-Reyes, C. M. Quiroa-Montalván, L. Cruz-López, A. Lenoir, and J.-P. Lachaud. 2015. How to escape from the host nest: imperfect chemical mimicry in eucharitid parasitoids and exploitation of the ants hygenic behavior. J. Insect Physiol. 75: 63–72.

Ronquist, F., and J. P. Huelsenbeck. 2003. MRBAYES 3: Bayesian phylogenetic infrerence under mixed models. Bioinformatics 19: 1572–1574.

Stamatakis, A., P. Hoover, and J. Rougemount. 2008. A rapid bootstrap algorithm for the RAxML web servers. Syst. Biol. 57: 758–771.

Swofford, D. L. 2002. PAUP*. Version 4.0 ß10., vol. Sinauer, Sunderland, MA.

Wheeler, W. M. 1907. The polymorphism of ants with an account of some singular abnormalities due to parasitism. Bull. Am. Mus. Nat. Hist. 23: 1–108.

Received 15 January 2015; accepted 12 June 2015.